LA-UR-22-20555

Approved for public release; distribution is unlimited.

Title:	Source Physics Experiment 3 (SPE3) - RV/DC Task 1.3 FY22 Final Report Legacy surface change analyses of the 1993 Rock Valley earthquake sequence for direct comparison to planned NA-22 underground conventional high-explosive experiments
Author(s):	Pope, Paul Albert Schultz-Fellenz, Emily S. Crawford, Brandon Michael Milazzo, Damien Michael Coats, Dane Erik
Intended for:	Completion of project task and reporting to customer
Issued:	2022-01-24

Source Physics Experiment 3 (SPE3) - RV/DC Task 1.3 FY22 Final Report

Legacy surface change analyses of the 1993 Rock Valley earthquake sequence for direct comparison to planned NA-22 underground conventional high-explosive experiments

January 20, 2022

Paul Pope, ISR-2
Emily S. Schultz-Fellenz, EES-14
Brandon Crawford, EES-14
Damien Milazzo, EES-14
Dane Coats, EES-14

BACKGROUND

Introduction

Recent work under two previous phases of the NNSA NA-22 Source Physics Experiment (SPE) have shown that underground chemical high-explosive experiments can produce detectable surface changes that differ in spatial extent and vertical magnitude depending on the geologic media at the site (Schultz-Fellenz et al., 2018; 2020; Crawford et al., 2021). Neither of these two prior phases of SPE identified natural earthquake-related surface effects in the same region that occurred at a similar depth as the explosive experiments for direct comparison. While earthquakes can also produce surface changes that are detectable using remote sensing data analyses, it is expected that the pattern and spatial extent of surface changes would vary between earthquakes and explosions. However, no direct-observed surface-change signature comparison between earthquakes and explosions has ever been performed.

The SPE Phase 3 Rock Valley/Direct Comparison (RV/DC) program presents a unique opportunity to investigate and characterize co-occurrence of both earthquakes and explosions. In this project, we worked to address five tasks in a workflow, as follows:

1. Identify and obtain existing high-resolution legacy satellite and aerial imagery as close in time before and after the 1993 Rock Valley earthquake sequence to temporally constrain the analyses.

2. Transform these pre-earthquake and post-earthquake datasets into digital elevation models (DEMs) using geospatial analysis software packages (e.g., ArcGIS, Agisoft Metashape, and Google Earth Engine).

3. Perform DEM differencing analyses to assess and quantify earthquake-related changes from the 1993 sequence, and develop map products that visualize these analyses.

4. Use the analyses from (3) to

   (a) assess spatial distribution and magnitude of surface changes due to the 1993 Rock Valley earthquake sequence, and
   (b) determine parameters of forthcoming, planned explosion-related surface change data collection from sensors mounted on unmanned aerial vehicles (UAVs) (e.g., spatial extent of collection, design and density of survey control, sensors to deploy, forward speed and line spacing of UAV flight lines, flight altitude).

5. Develop a summary report on the analyses, including how the analyses define parameters and identify focus areas for any future surface change analytical field campaigns related to the explosive experiment.

Analyzing these legacy data and identifying whether they can detect any surface changes related to the earthquake sequence facilitates opportunities for direct signature comparison of surface change from explosions at one location, which has never previously been performed. Comparing the surface change signatures from a co-located and depth-equivalent earthquake and an explosion could help to advance remote sensing event discrimination techniques. This report summarizes the work completed toward this ambitious goal.

Rock Valley Nevada Test Site Very Shallow Earthquake Sequence

In mid-1993, a sequence of unusually shallow earthquakes (i.e., a depth of less than 3 kilometers) occurred in the Rock Valley fault zone, located at the southern end of the Nevada Test Site within Area 27 (Fig. 1). The largest earthquake event, which occurred on May 31, 1993, was 3.7 in magnitude (Table 1). Over a 5 month period, 140 other events triggered the local short period seismic network, and there were approximately another 500 smaller earthquakes (Smith et al 2000).

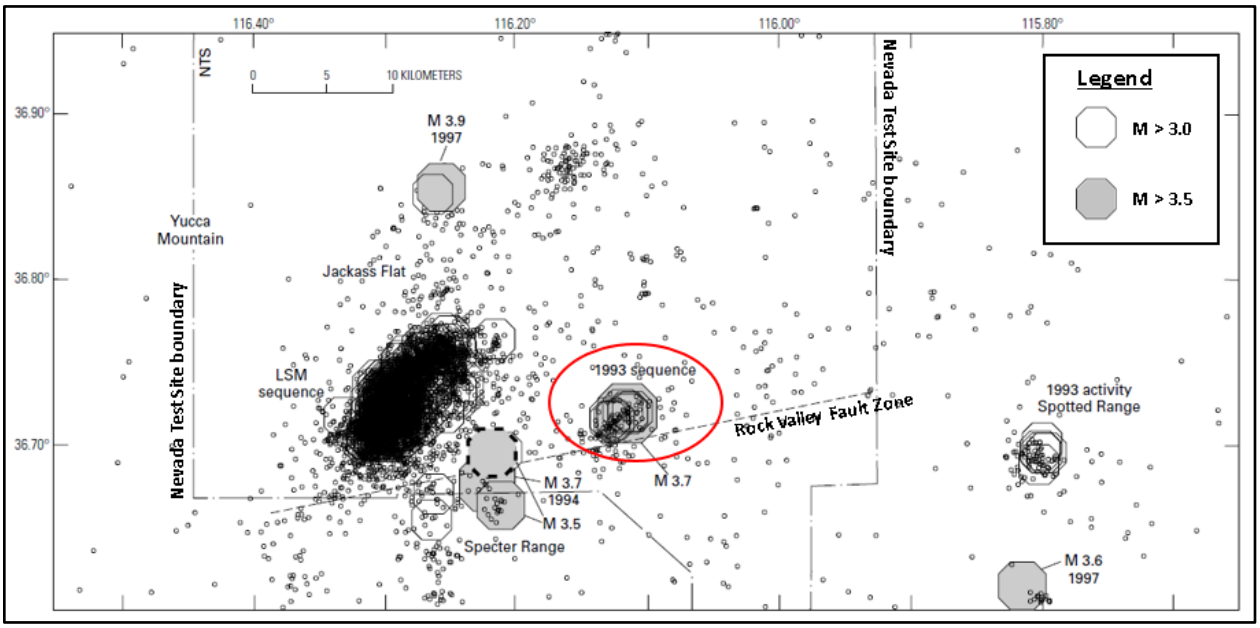

Figure 1. *Earthquake event locations at the southern end of the NTS including the 1993 sequence (circled in red) that defines the study area for this work. (Smith et al. 2000; Fig. 3 modified)*

Table 1. The 1993 earthquake sequence characteristics, including time, location, depth (Z), and magnitude. (Smith et al. 2000; Table 1 modified)

EV#	Origin time	Latitude (°N.)	Longitude (°W.)	Z	M_W
1	93 530 1520 62.49	36 43.11	116 06.95	2.06	3.7
2	93 531 315 79.97	36 43.23	116 07.17	1.91	2.4
3	93 531 918 49.14	36 42.98	116 07.86	2.37	2.6
4	93 531 1113 67.99	36 43.41	116 06.66	1.86	2.1
5	93 531 1244 72.78	36 43.32	116 06.78	2.25	2.9
6	93 531 2238 47.40	36 43.32	116 07.09	1.84	2.0
7	93 6 1 1628 65.15	36 43.21	116 06.95	1.68	2.8
8	93 6 3 835 70.40	36 43.37	116 06.51	0.71	2.2
9	93 6 3 1720 32.89	36 42.96	116 07.49	1.80	2.4
10	93 6 4 1623 37.38	36 43.22	116 08.18	0.85	2.0
11	93 6 5 1323 71.33	36 42.89	116 07.67	1.63	2.5
12	93 6 6 1531 43.82	36 43.22	116 06.93	2.45	2.5

Surficial Expressions and Remote Sensing Modalities

The application of remote sensing techniques to geomorphology and geomorphic change detection has been employed since the late 1970s, with the availability of Landsat data (e.g., Smith and Pain, 2009 and references therein; Tarolli and Mudd, 2020). There are several phenomena induced by relatively shallow earthquakes and explosions that could be evident as surface geomorphic change within remotely sensed data. Vertical and horizontal (thrust and strike-slip, respectively) ground motion could result in non-elastic displacement (shifts) along previous faults, and/or result in activation and detection of new faults represented as surface rupture (e.g., Fan et al., 2019). Radar and lidar modalities might be able to discern these shifts. For signature discrimination and event attribution, submeter precision would most likely be required. Broad-scale surface subsidence and/or uplift might also be expected, requiring the same remote sensing modalities and spatial precision. Such changes were observed and quantified during investigations of individual underground conventional high-explosive experiments in SPE Phases 1 and 2 (Schultz-Fellenz et al., 2018; 2020; Crawford et al., 2021); it is important to note that the surface morphologic changes detected in these studies were decimeter to sub-decimeter scale. Landslides of loosened talus, and surficial scars left by tumbling boulders (Fig. 2) might also be expected, and in some instances may span a large spatial area depending on the local geologic conditions and rupture (e.g., Kargel et al., 2015). Spatial precision on the order of a meter would be required. Radar and lidar, as well as natural color and color infrared (CIR) imagery, as acquired by aerial or satellite platforms, have been used to discern these effects. While it is assumed that surface geomorphic signatures of earthquakes may have linear correlation to a fault trace or be proximal to an epicentral location, those signatures may be controlled by the rock types present in the area of interest, which could limit or extend their distribution.

Figure 2. *Example of a precarious rock, located approximately 10 km south of Yucca Mountain (Brune and Whitney 2000; Fig. E).*

METHODOLOGY

In order to effectively and accurately use remotely sensed data to detect surficial expressions of near-surface historical seismic events, the initial focus was on the 1993 earthquake sequence (Table 1). The general steps in the methodology were (1) obtaining remotely sensed data before and after the earthquake sequence, (2) co-registering these data, and (3) performing analyses to detect surficial change. This work proceeded in two phases. The first phase was exploratory in nature, mainly to ascertain whether there were any detectable changes whatsoever within the historical aerial photography, and aimed at accomplishing tasks 1 and 2 in the workflow and proposed scope. Because this initial work was successful, a second phase was pursued whereby more complicated methods were used to align the historical aerial photography, thus driving towards achieving tasks 3 and 4 in the workflow and proposed scope.

Remotely Sensed Data

The USGS Earth Explorer was used to search for radar, lidar, and aerial imagery of the study area (Fig. 3) acquired before and after the 1993 earthquake sequence. Only eight National Aerial Photography Program (NAPP) aerial photos (circa 1994) were available, and unfortunately they did not include all of the area of interest, only its most southern portion. Satellite imagery was also searched for via the Digital Globe (Maxar) Global Enhanced GEOINT Delivery (G-EGD) platform tool. This effort also resulted in no matches. This paucity of data was most likely due to the fact that remotely sensed imagery exhibiting a fine spatial resolution (i.e., less than 10m) of the former NTS is sensitive with regards to national security.

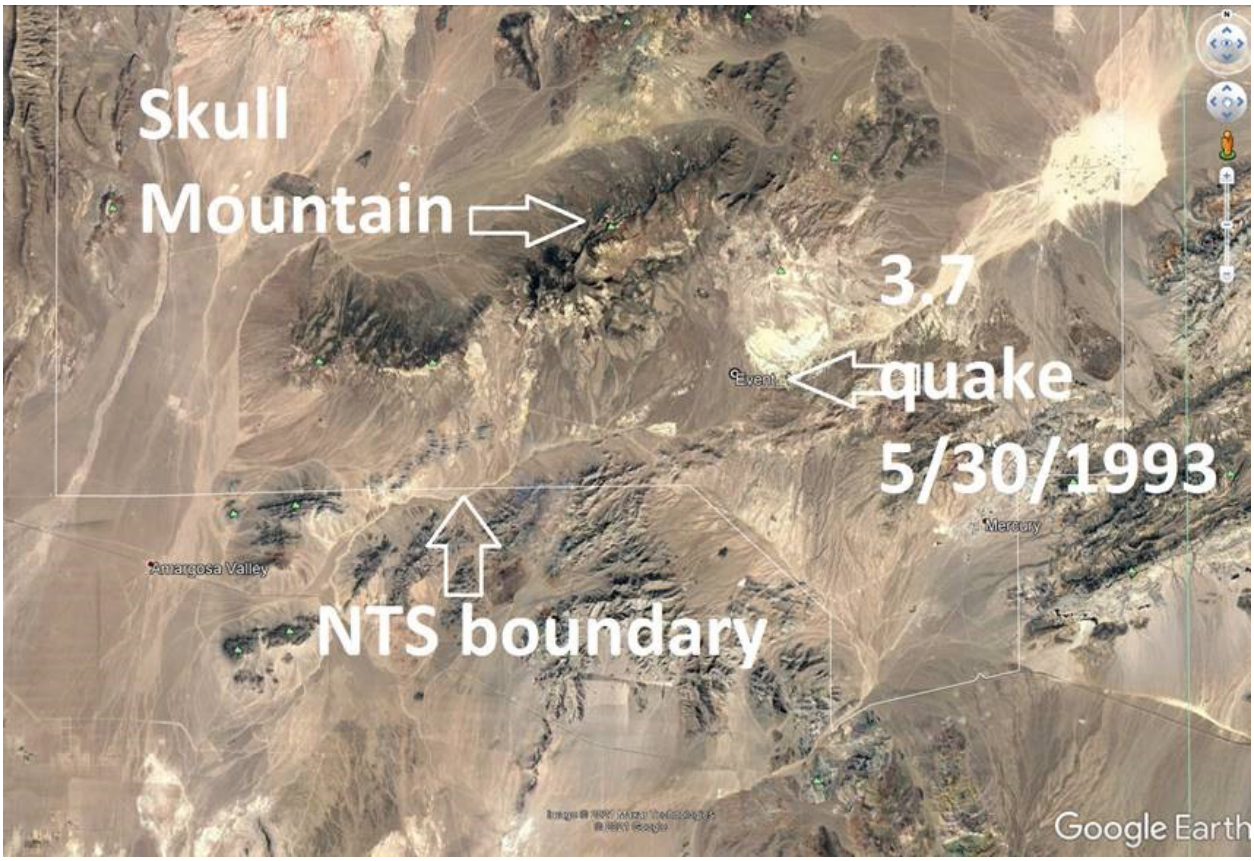

Figure 3. *Satellite image of the study area (image © 2021 Maxar Technologies) overlaid with features of particular relevance to this study. Rock Valley runs diagonally through the center.*

Therefore, staff at the management and operating contractor for the current NNSS, Mission Support and Test Services (MSTS), were contacted to solicit their assistance in locating and acquiring legacy or historic remotely sensed data of the study area. Specifically, the DOE's Remote Sensing Lab (RSL), located at Nellis Air Force Base, Las Vegas, Nevada, was approached. This collaboration was very productive. Aerial photographs (on rolls of film media) from before (July 19, 1986) and after (August 28, 1994) the 1993 earthquake sequence were located in archival storage, digitized, and electronically delivered to LANL by RSL-Nevada (Table 2) in July of 2021. An Epson Expression 10000XL flatbed scanner was used to perform

the digitization. The maximum optical resolution of 2400 dots per inch (dpi) was used. The bit depth was set to 16 bits per pixel for each of the three color bands (red, blue, and green). The output format was TIFF.

Table 2. Metadata of the "before" and "after" frames of aerial photography.

Acquisition Date	Scale	Roll # - Frame #	GSD_Avg.[meters/pixel]
July 19, 1986	1:57,700	5373-71	0.61
July 19, 1986	1:57,700	5373-72	0.61
July 19, 1986	1:57,700	5373-73	0.61
August 28, 1994	1:32,000	7876-80	0.34
August 28, 1994	1:32,000	7876-81	0.34
August 28, 1994	1:32,000	7876-82	0.34

Phase 1: Georegistration and Layer Stacking

Two frames were selected for analysis; 5373-72 ("before") and 7876-81 ("after") (Fig. 4). USGS Digital Ortho Quarter Quads (DOQQs) covering the study area (Fig. 5) were downloaded via the USGS EarthExplorer and used for planimetric (horizontal) ground control. Ground control points (GCPs) were manually set between each of the two frames and the DOQQs; 137 GCPs for frame 5373-72 and 93 GCPs for 7876-81. Shrubs provided excellent features for setting GCPs due to their point-like characteristic, high contrast, and persistence (Fig. 6). The Coordinate Reference System (CRS) was UTM Zone 11 North (NAD83 datum). An affine transformation was used to resample each frame to the CRS. The spatial overlap between each frame as compared to the USGS DOQQ "Camp Desert Rock NW" was used to bound the extent of the resampling output. The ground sample distance (GSD) was the same as the USGS DOQQ, that is 1 meter per pixel. The RMSE was 29 pixels for the "before" image and 44 pixels for the "after" image. The resampled "before" and "after" frames were output to a single raster ("layer stack") to facilitate change analysis via visual interpretation (Fig. 7).

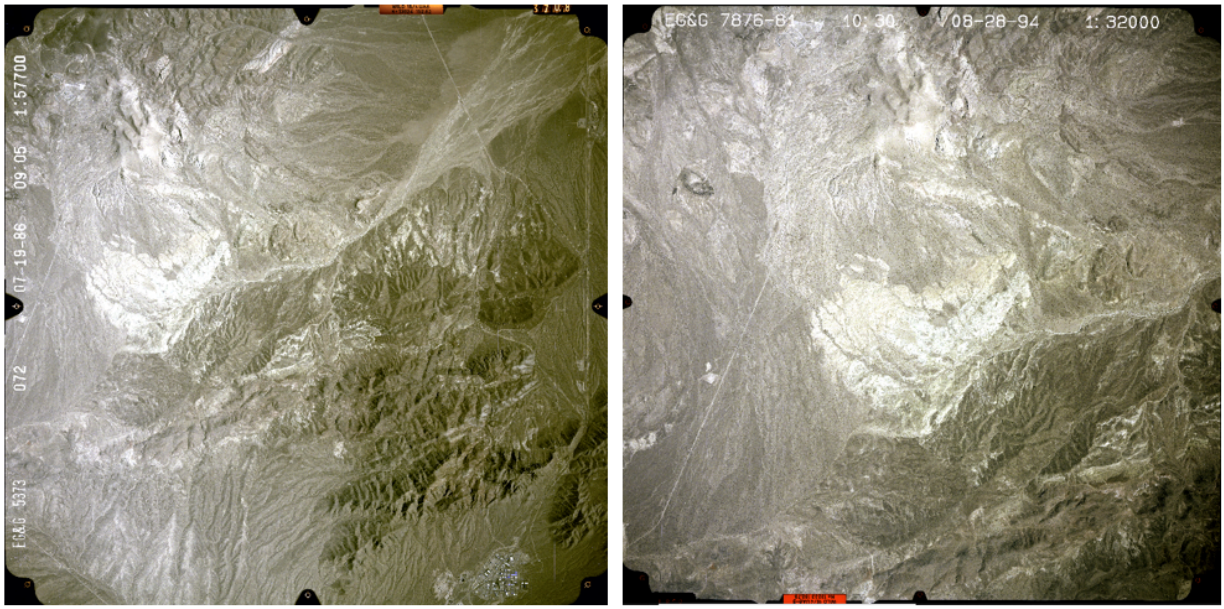

Figure 4. *The (a) "before" (GSD of approximately 4m/pixel) and (b) "after" (GSD of approximately 2m/pixel) frames.*

Figure 5. *Names and boundaries of the USGS Digital Ortho Quads (DOQs) which cover the study area. Each DOQ consists of four DOQQs ("NW," "NE," "SE," and "SW"). Location of the 3.7M earthquake on May 30, 1993 is shown as "Event_1."*

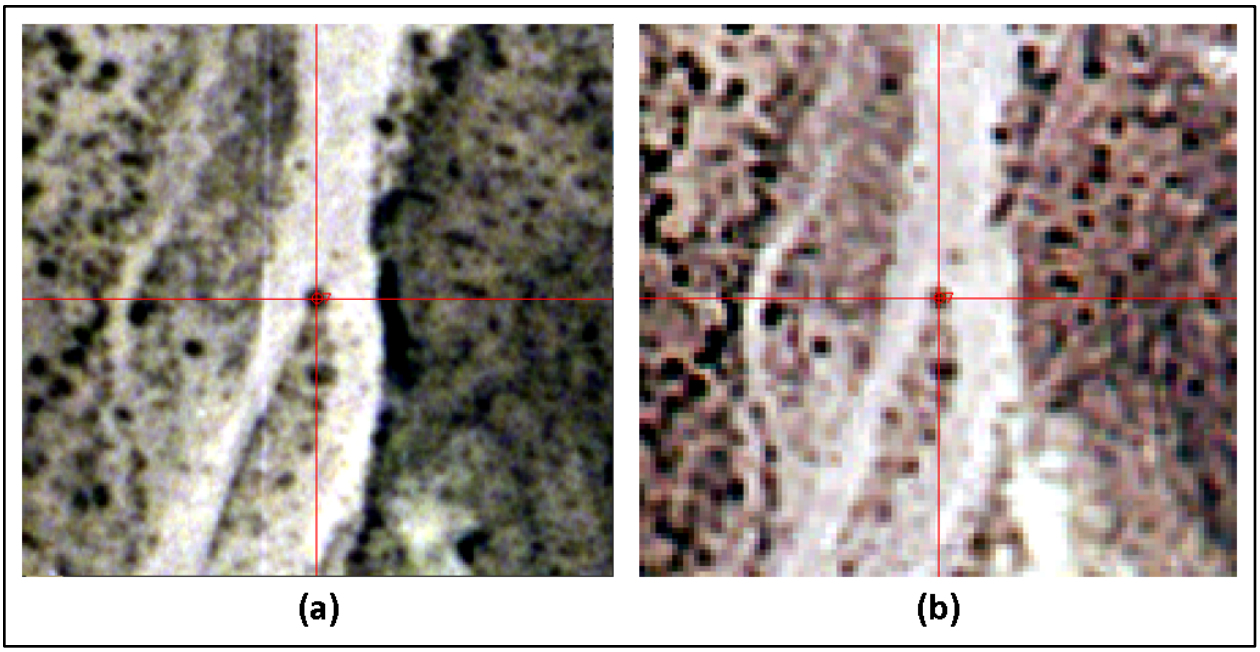

Figure 6. *Example of conjugate point selection by using a shrub as a GCP (a) as it appears in the "after" image (2X zoom) and (b) as it appears in the USGS DOQQ "Camp Desert Rock NE" (4X zoom).*

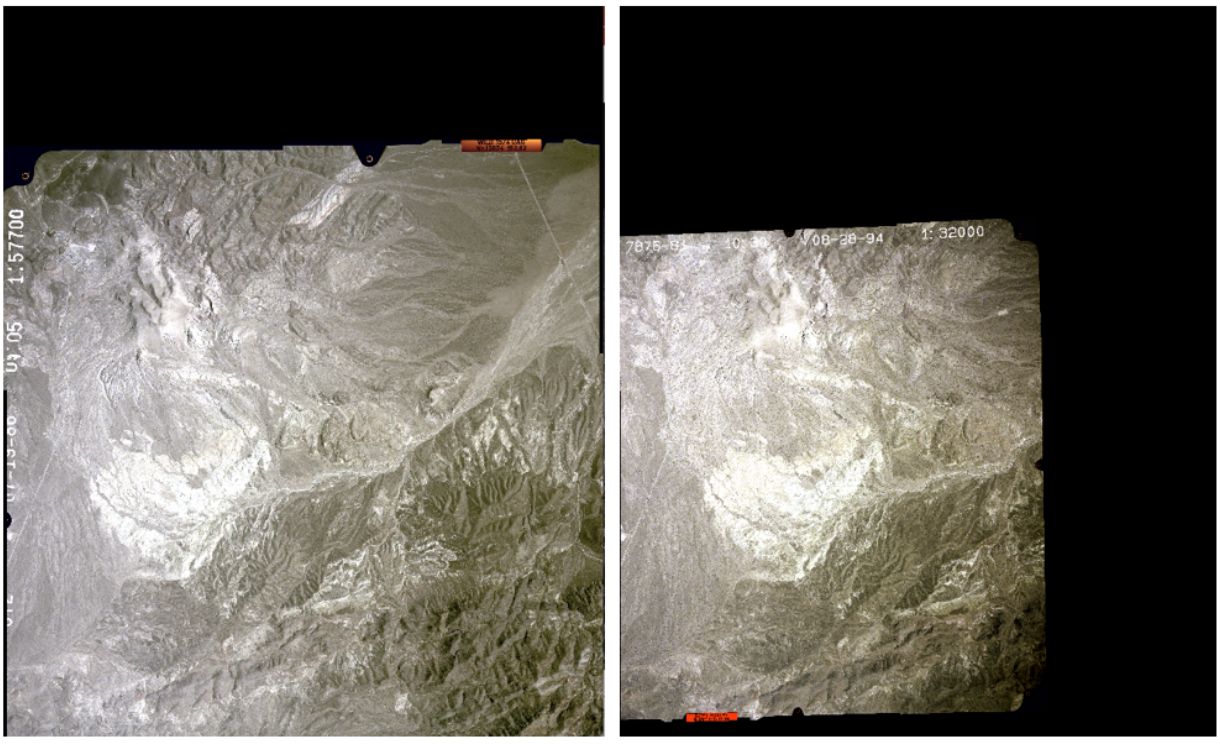

Figure 7. *The (a) "before" and (b) "after" frames produced by resampling the original imagery (Fig. 4) to a common CRS, extent, and GSD as defined by the USGS DOQQ "Camp Desert Rock NW." The black areas are "padding" due to incomplete overlap in coverage as compared to the DOQQ.*

Phase 1: Visual Interpretation of Layer Stack

The layer stacked "before" and "after" images (red band only) were displayed in a single view and flickered so that localized change could be detected through visual inspection. The imagery was inspected by using a raster search pattern. The change of interest was from a dark tone to a light tone, implying that a fresh surface of a rock or other geologic feature was newly exposed due to motion or movement. A marker (annotation; pin) was placed over these visually detected changes.

Phase 1: Results

Two hundred and seventy nine (279) surficial change candidates were detected and annotated via visual inspection and on-screen digitizing (Fig. 8). Many of the 279 changes detected were "false positives", or changes between image frames that were attributed to dust, lint, and scratches on the original film photograph. Although great care was taken in digitizing the frames, film is prone to these phenomena and so they cannot be completely eliminated. Another source of "false positives" were splotches and flecks of white ink, especially near the metadata (e.g., time, date, frame number, etc.) that are printed directly upon the photography.

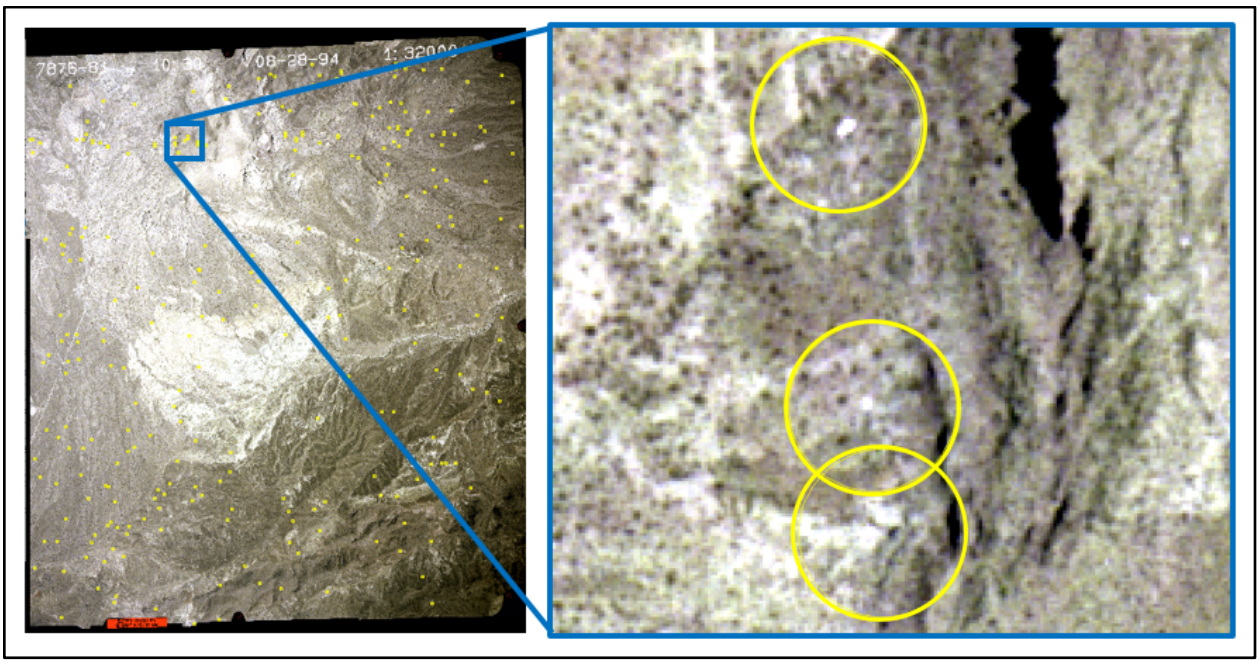

Figure 8. *The 279 surficial change candidates (yellow points) overlaid on the georegistered "after" image. The inset shows details of three examples.*

Visual inspection was an effective albeit laborious method, even with the pervasive changes that had to be "overlooked," such as differences in lighting, shifts due to parallax, and differences in optical resolution (Fig. 9).

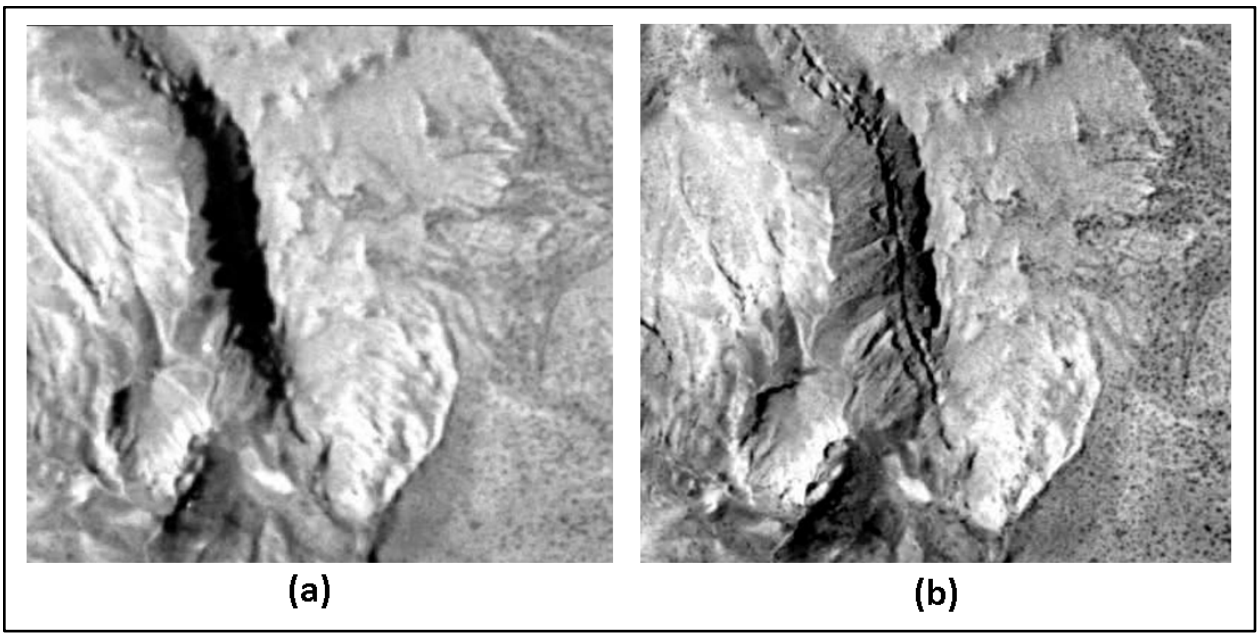

Figure 9. *Example of pervasive change (e.g., shadow, parallax, and optical resolution) between the (a) "before" and (b) "after" imagery.*

Some of these 279 annotations are almost certainly actual surficial changes (i.e., "true positives"). There were some (approximately twenty) whose shape, tone, and context (e.g., within a scarp) that would be logically consistent with features produced by, for example, localized talus gravel or path effects following the downhill descent of a dislodged boulder.

To summarize, Phase 1 included the completion of task 1 (identify and obtain existing legacy imagery before and after the 1993 Rock Valley earthquake sequence), and partial completion of task 2 (digital transformation of the pre-earthquake and post-earthquake datasets) from the workflow proposed in the original work scope.

Phase 1 transition to Phase 2

The success of the Phase 1 study prompted a more rigorous analysis of the historical imagery, specifically the application of photogrammetric techniques. The impetus for continuing on to a Phase 2 study was two-fold. First, orthorectification was expected to greatly improve the spatial accuracy of the location of the surficial change candidates. Second, the large overlap between the aerial photography was expected to aid in eliminating any false positives due to dust, flecks of paint, etc. on the film via reciprocity (that is, features on the ground should be apparent from both camera viewpoints).

Phase 2: Bundle Adjustment

A bundle adjustment was performed on four of the six historical aerial photographs, specifically 5373-71, 5373-72, 7876-81, and 7876-82 (see Table 2). The bundle adjustment calculation

determined the position and orientation of the camera at the instant each photograph was taken. The focal length of 156 millimeters was known from the flight logs associated with both acquisitions. Ground control points (GCPs) were set by using the DOQQ imagery to identify conjugate points. The height of each GCP location was determined by using the USGS ⅓ arc-second (approximately 10 meters per cell) Digital Elevation Model (DEM) for the study area (Fig. 10). Once the bundle adjustment was completed, the footprint of each aerial photograph could be created for reference purposes (Fig. 11).

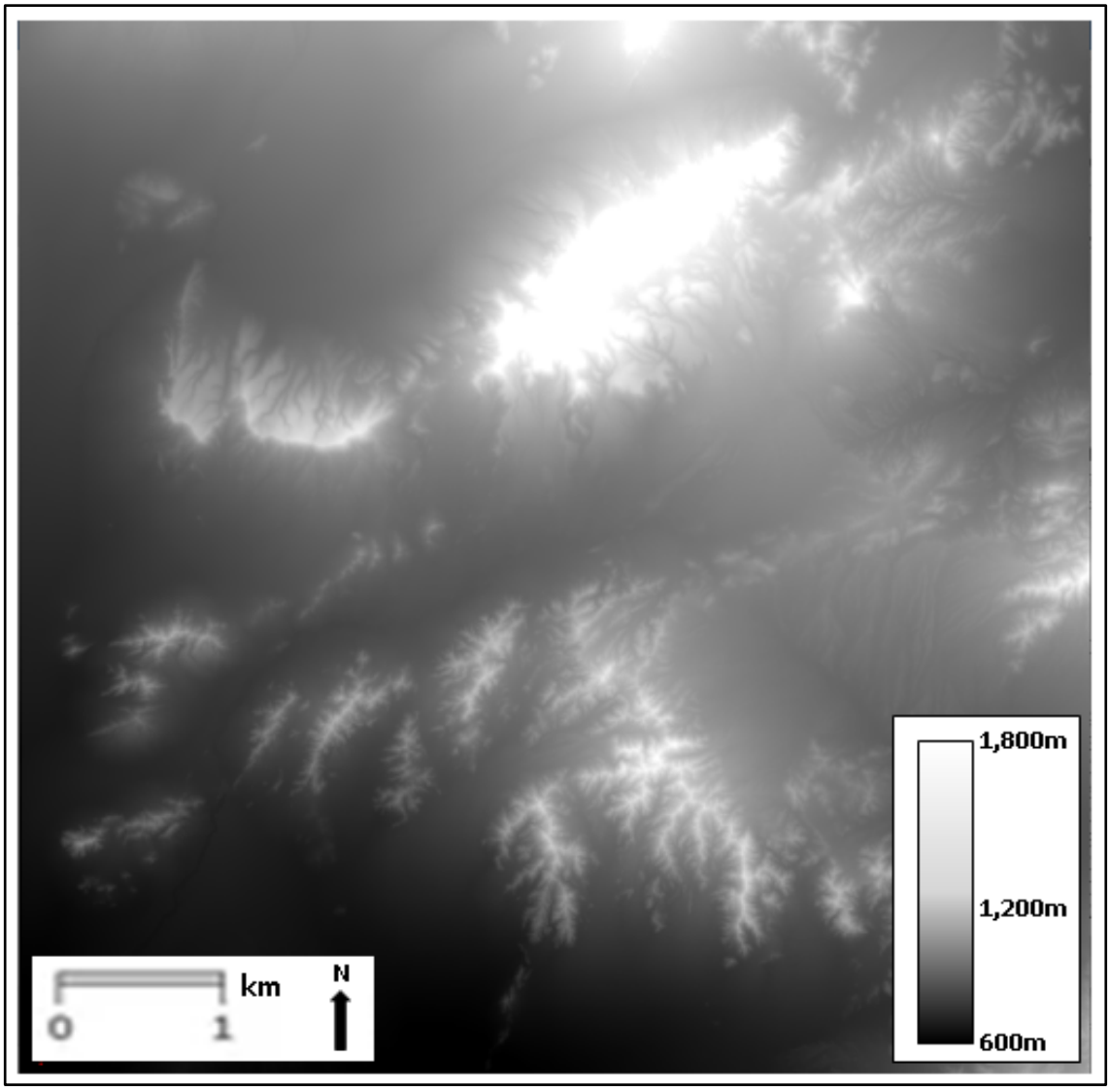

Figure 10. *The USGS ⅓ arc-second DEM for the study area. Rock Valley runs diagonally from west-southwest to east-northeast through the center of the figure. Heights are above MSL.*

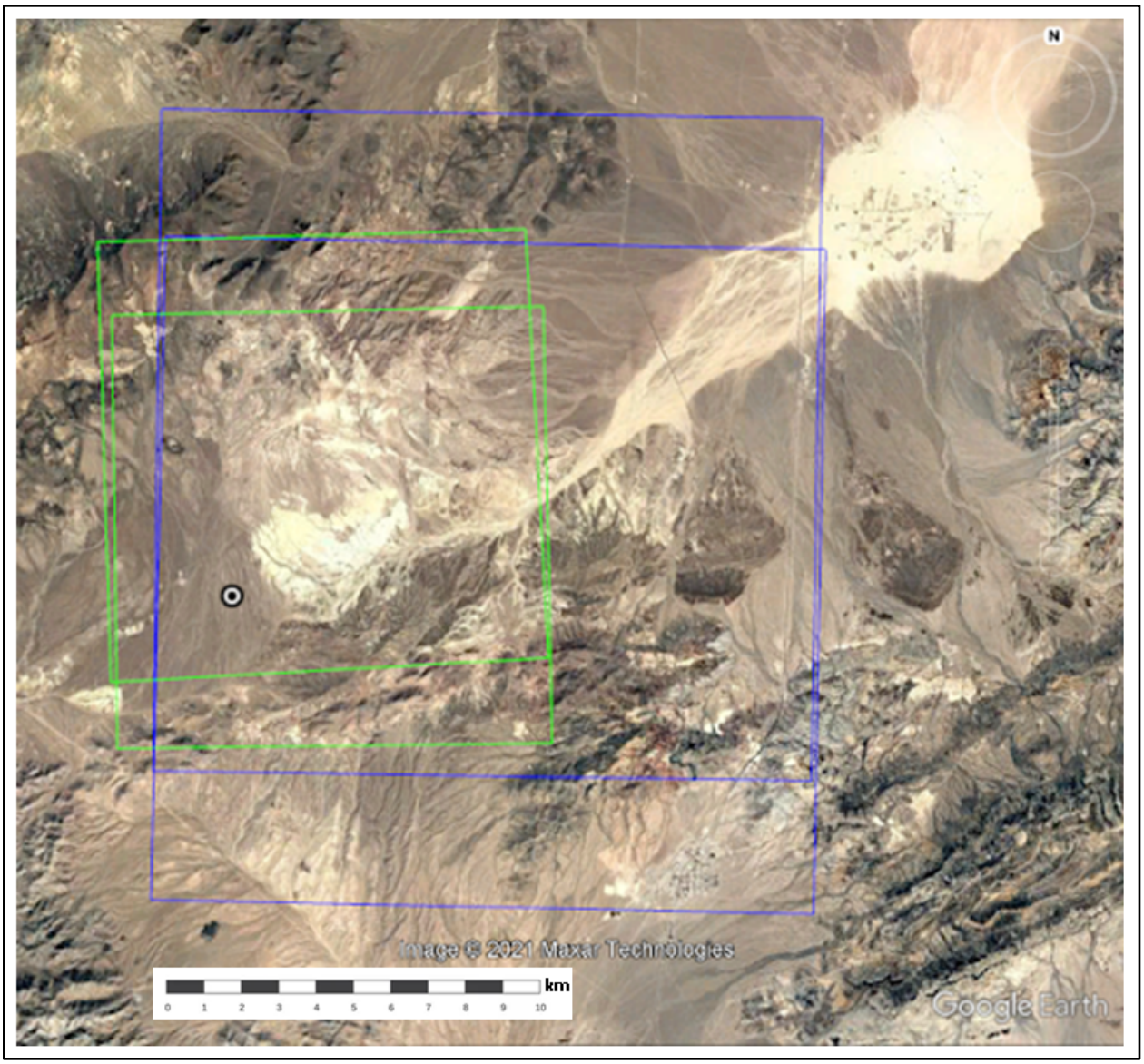

Figure 11. *The footprints of all four aerial photographs. The two footprints for the 1986 acquisition (5373-71 and 5373-72) are shown as blue squares, the two footprints for the 1994 acquisition (7876-81 and 7876-82) are shown as green squares, and the location of the 3.7M earthquake is shown as a point. Note the significant forward overlap (~80%) that is typical of aerial survey photography. (background image © 2021 Maxar Technologies)*

It should be noted here that the bundle adjustment accuracy was limited by two factors. First, the cell size of the DEM was an order of magnitude greater than that of the DOQQs that were both used to define the GCPs used as input to this photogrammetric process. Therefore, the bundle adjustment solution accuracy was approximately +/- 20 meters (95% CI) for all four photos. Second, the bundle adjustment residuals, as projected onto the focal plane of the aerial mapping camera strongly suggest that the film is suffering from shrinkage, a common phenomena that is characteristic of physical media (Fig. 12).

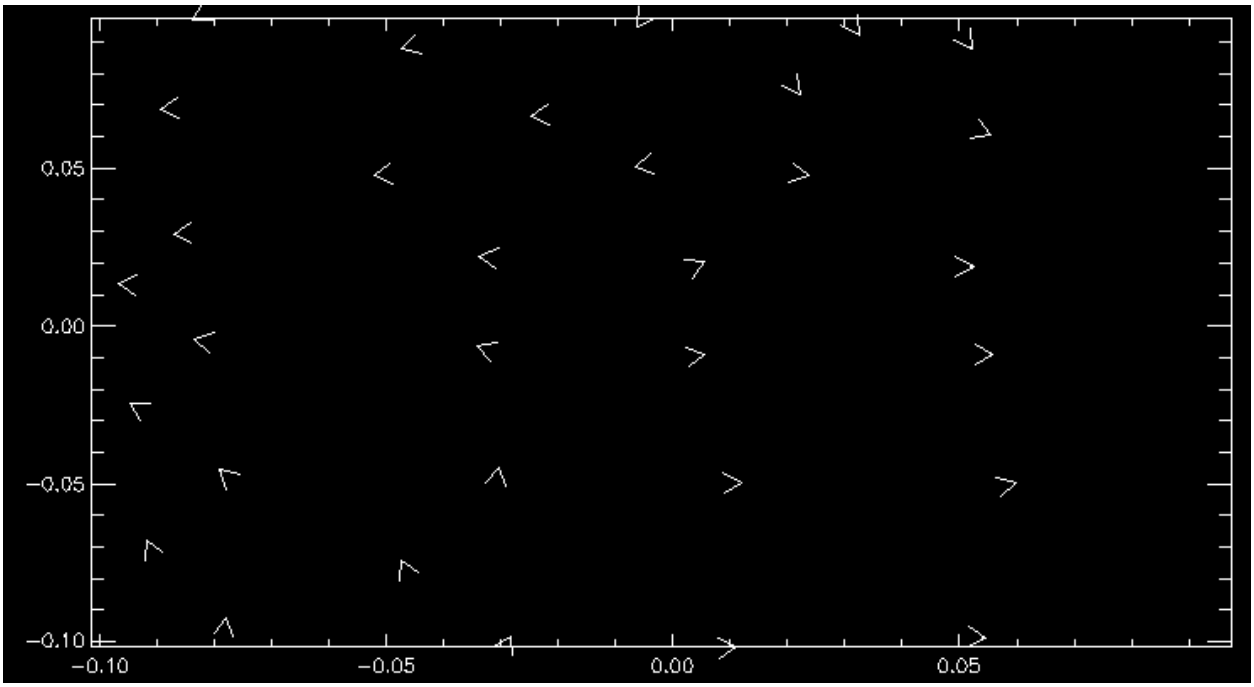

Figure 12. *Bundle adjustment residuals (roll-frame # 5353-72), as projected onto the focal plane of the aerial mapping camera. The general trend, from a central vertical line out toward the left and right edges, strongly suggests that the film (a long roll) is suffering from shrinkage, and does not represent actual lateral shifts of the ground surface away from a plane oriented north-south, projecting up from the 0.00 mark on the x-axis.*

Phase 2: Orthoimage Creation

Next, the photogrammetric process of orthorectification (differential rectification) was used to create an orthoimage for each of the four historical aerial photographs. Orthorectification removes distortions due to both aerial camera tilt as well as terrain relief. The bundle adjustment solution and the DEM were the two main inputs to this process. The same output cell size (1 meter) and geographic extents (region of interest) were used to create each of the four orthoimages (Fig. 13). The coordinate reference system (CRS) was UTM Zone 11N based on the WGS84 datum.

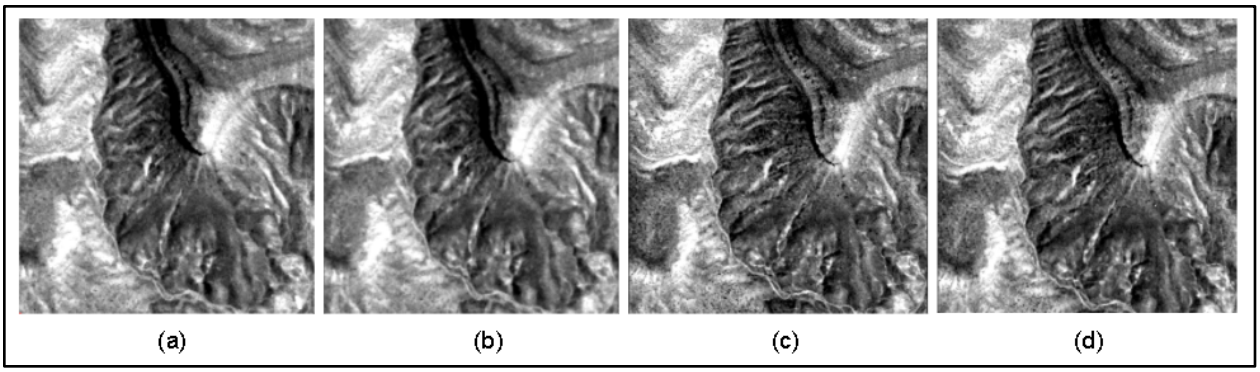

***Figure 13**. The advantages of orthorectifying the historical imagery are evident via this montage of subsets of the orthoimagery created from the 1986 aerial photographs ((a) 5353-71 and (b) 5353-72) and the 1994 photographs ((c) 7876-81 and (d) 7876-82). Differences due to scale, orientation, perspective (tilt), and terrain relief have been largely compensated for, thereby facilitating the discovery of surficial change candidates through visual inspection. These orthoimage subsets are 400m by 400m in size each and North is toward the top.*

Phase 2: Visual Interpretation of Orthoimagery

The four orthoimages were arranged and displayed side-by-side to facilitate comparison. Flickering between the “before” and the “after” imagery was used to perform visual inspection to identify surficial change candidates by looking for localized dark to light changes. False positives due to dust, flecks of paint, etc. were eliminated by comparing the two “after” orthoimages to ensure that the suspected change feature was detectable in both images. The heavy forward overlap between the aerial photographs facilitated this consistency check (Fig. 14). If a detected change was found to be consistent, then a marker (annotation; pin) was placed over the surficial change candidate as it appeared in the orthoimage. The imagery was visually inspected by using a raster search pattern.

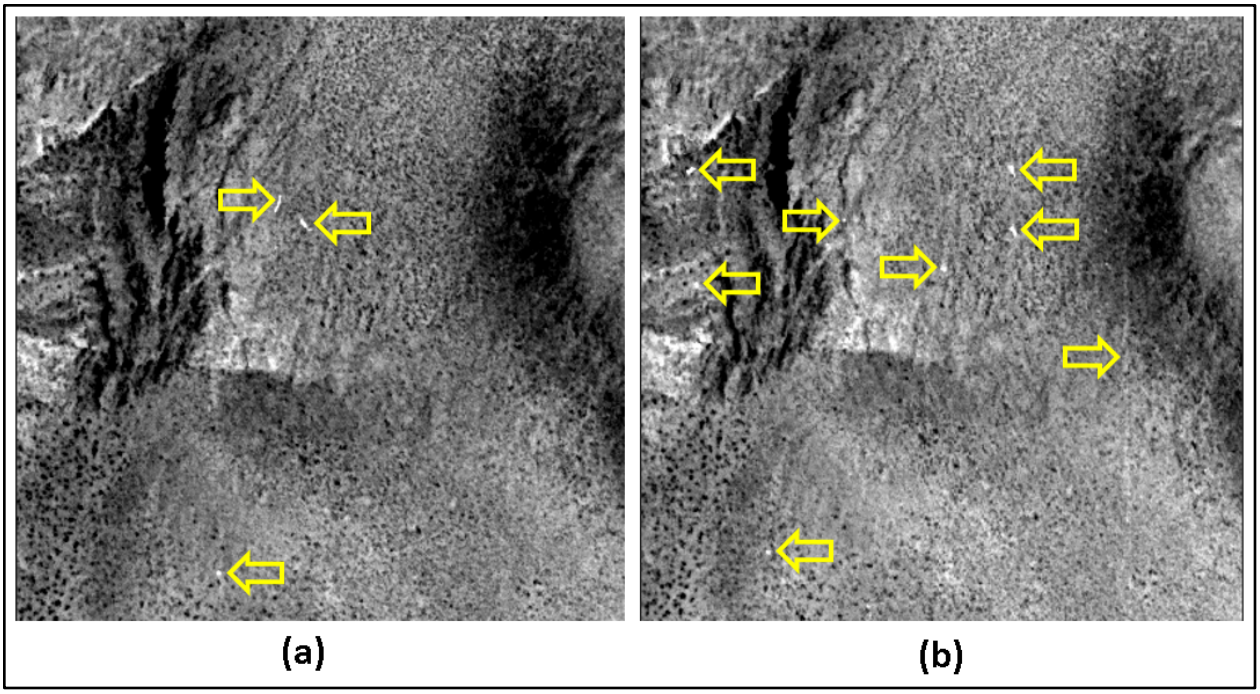

***Figure 14**. Example of how multiple false positives are eliminated by leveraging the reciprocity provided by the heavy overlap between the "after" frames of aerial photography ((a) 7876-81 orthoimage and (b) 7876-82 orthoimage). Specifically, light toned features on one frame do not appear on the other, which provides a strong indication that the feature is not on the ground, but rather contamination or scratches etc. on the film. These orthoimage subsets are 400m by 400m in size each and North is toward the top.*

Phase 2: Results

One hundred and thirteen (113) surficial change candidates were detected and annotated (Fig. 15). Since the region of interest between the phase 1 and phase 2 efforts were essentially the same, this implied that making use of the reciprocity afforded by the heavy overlap between aerial photography frames reduced the number of false positives due to film contaminants by approximately 60%.

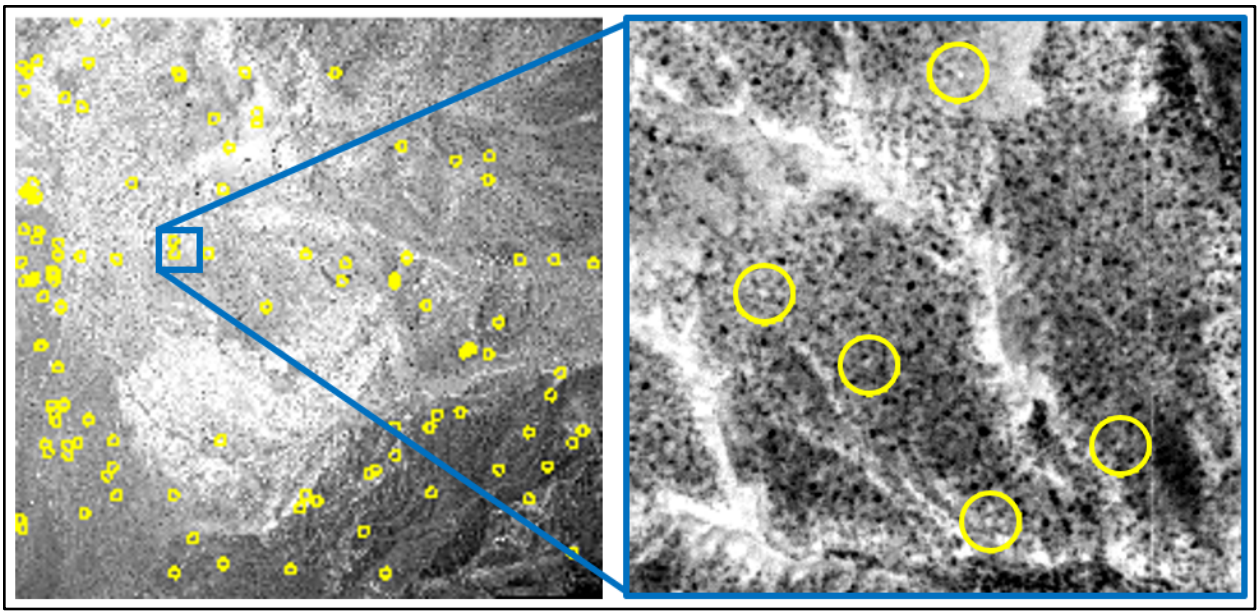

Figure 15. *The 113 surficial change candidates (yellow points) overlaid on the orthorectified "after" image (7876-82). The inset shows detail of five examples.*

Fig. 16 illustrates the results from a geospatial analysis that combines terrain, geologic, and geophysical information with the 113 surficial change candidates derived from this study's visual interpretation of the orthoimagery, to highlight the intersection of high slope areas, rocky geology, and identified legacy aerial image surface changes alongside known faults within Rock Valley.

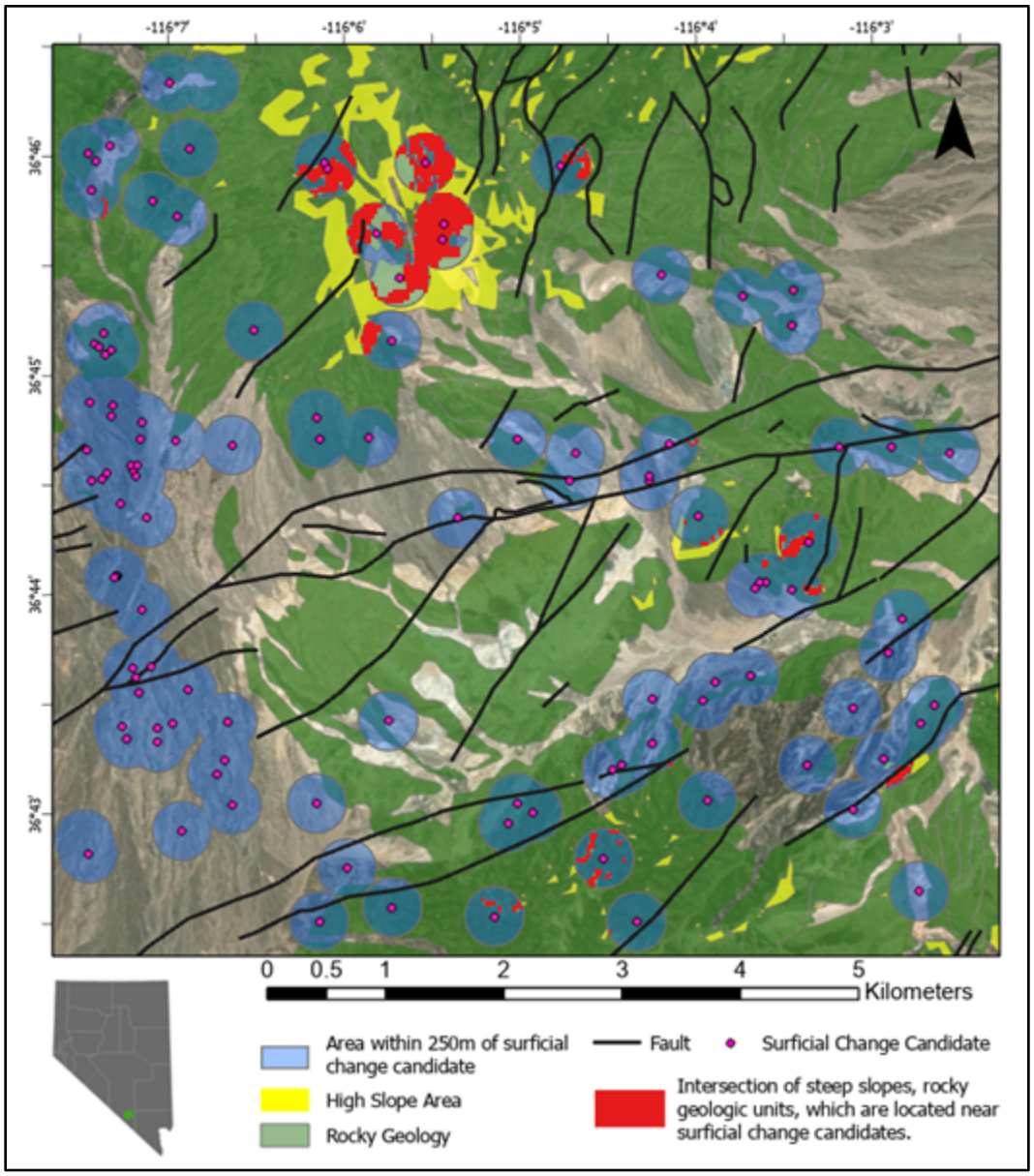

***Figure 16**. Example of a map based on geospatial analysis that could be used to prioritize field investigation of the surficial change candidates.*

From this overlap of surficial change candidates, geologic boundaries, and slope areas we identified 5% of the change candidates overlap with all variables, 7% overlap with slope, 43% overlap with geology, and 59% overlap with no underlying variables (Table 2). From this we see there is a limited correlation between surficial change candidates and slope (7 points), which could be related to the general topography of the valley. Likewise, we do not identify many locations (6 points) where changes were identified in both a high slope and geologically pertinent layers. Our second strongest relationship appears to be between underlying geology and identified change locations (43 points). This stronger correlated relationship could be caused by the presence of precarious rocks (Fig. 2), media susceptible to ground motion, other factors, or there are unidentified causations for this relationship. Finally, our strongest correlated

relationship is between change candidates and no underlying factors (65 points). These points are concentrated within the alluvial basin and may be longer term deformation occurring over the 6 year period between image collection. Investigating these locations will be essential to understanding what changes within these basins, and whether they can be identified at higher resolutions. Understanding of this relationship between slope, geology, and detected change will be essential to discerning surficial change during RV/DC. This preliminary work will drive field investigations and modern imagery collection, for later post experiment comparison, to further compare and distinguish earthquake from underground testing signals

Table 2 : Correlation of surficial change candidates with other GIS parameters.

Name	**Count**	**% of total points**
No intersection	65	59%
Geology	43	39%
Steep Slope	7	6%
Geology + steep slope	6	5%

To summarize, Phase 2 included the partial satisfaction of task 3 (perform differencing analyses to assess earthquake-related changes from the 1993 sequence, and develop map products that visualize these analyses), and completion of task 4 (assess spatial distribution of surface changes, and use these data to inform forthcoming, planned explosion-related surface change data collection from sensors mounted on unmanned aerial vehicles (UAVs).

DISCUSSION and FUTURE WORK

The Phase 1 work verified that there is in fact remotely sensed evidence of surficial change that is consistent with what would be expected due to material movement induced by earthquake activity, specifically a change in tone from dark to light as the surface is disturbed (e.g., boulder rolling downhill). Given that success, Phase 2 work was performed to increase the location accuracy of the surficial change candidates and to eliminate false positives due to film contamination. Through the course of the execution of work, it became clear that certain scope elements were not going to be achievable in the remaining budget and timeframe of the project, and as such were tabled for future consideration. These include: development of digital elevation models (DEMs) from the pre-earthquake and post-earthquake orthoimagery, and quantification of change detected in the image analyses (which requires the DEMs to accomplish). The study produced a valuable location assessment of changes and qualitative

review of the possible signatures represented in the change detection. The data have been provided to the LANL uncrewed aerial systems (UAS) team to develop, inform, and refine mission objectives and flight planning for forthcoming RV/DC baseline field characterization efforts. Furthermore, the results of this study will be discussed with SPE RV/DC working groups for community awareness and consideration.

With the current state of analysis and available project resources, this study was unable to complete analyses to determine the mechanisms that created the detected change. Future work will be required to execute additional analyses on the detected changes to ascertain if there are any patterns to them that are consistent with the source of the change being the 1993 earthquake sequence. Additionally, because the “before” and “after” imagery are separated by six years, other evidence provided via spatial association and pattern analysis should be pursued in order to bolster the argument for attributing any detected changes to the 1993 earthquake sequence and not to other geomorphic or natural processes.

Field work will be required in order to validate or refute these surficial change candidates, or some subsample thereof. However, it would be prudent to rank and prioritize these candidates before a field campaign is pursued to validate the results of this legacy data analysis. Filtering of the initial 113 candidates should be performed. Preference would be for candidates that are closest to the earthquake swarm and located on high slopes.

Masking, based upon geospatial analysis, could help prioritize attention to more competent geologic units (those that form rocky outcrops) and high slope areas, where talus and boulders are more unstable, as opposed to more level terrain. Additionally, regions either directly around faults or close to earthquake epicenters might justify preferential field inspection.
Finally, due to the laborious nature of visual interpretation and the large extent of the region of interest, digital change analysis should be pursued. This was not possible during the course of this study mainly because the coarseness of the USGS DEM (10 meters per cell) relative to the finer resolution of the historical aerial photography (sub meter per pixel) limited the planimetric accuracy of the orthoimagery (approximately +/- 20 meters). This limitation might be addressed by using photogrammetric techniques to create a finer resolution DEM (a substantial effort that was out-of-scope for this project), or possibly acquiring one from DOE-RSL or another government agency, assuming such a data source exists and is accessible.

CONCLUSION

This work has shown promise for detecting and highlighting some of the surficial effects before and after the 1993 earthquake swarm. Although limited, this work has identified that detectable change has occurred, and more importantly, there are changes which are retained and preserved for long periods of time. This is to say, the longer temporal extent of the datasets can also help in our understanding of the permanence of deformation and ground disturbance from the earthquake sequence. The pursuit of further photogrammetric processing and complementary geospatial analyses will allow for broader scale surficial change detection and characterization. This will also serve as an important dataset to compare this new venture to the

previous earthquake related deformation results. These are both potentially important datasets for discerning differences in surficial change from the earthquake sequence to complementary experiments.

ACKNOWLEDGEMENTS

The invaluable assistance of Steve Carragher and Irma Torres at DOE's RSL-Nevada is gratefully acknowledged. Their expertise, persistence, and "can do" spirit lead to the discovery and subsequent digitization and delivery of the remotely sensed data that made this initial work possible. We also thank Barbara Jennings and Cleat Zeiler of MSTS for their support to Steve Carragher and Irma Torres to develop this collaboration with LANL.

REFERENCES

Brune, J.N. and John W. Whitney (2000). "Precarious Rocks and Seismic Shaking at Yucca Mountain, Nevada," Chapter M, *U.S. Geol. Open---File Rept. Seismic Hazard Issues Yucca Mountain.*

Crawford B., E. Swanson, E. Schultz-Fellenz, A. Collins, J. Dann, E. Lathrop, and D. Milazzo (2021). A new method for high-resolution surface change detection: data collection and validation of measurements from UAS at the Nevada National Security Site, Nevada, USA. *Drones* **5**(2), 25, https://doi.org/10.3390/drones5020025.

Fan X., G. Scaringi, O. Korup, A.J. West, C.J. van Westen, H. Tanyas, et al. (2019). Earthquake-induced chains of geologic hazards: patterns, mechanisms, and impacts. *Reviews of Geophysics* **57** (2), 421-503, https://doi.org/10.1029/2018RG000626.

Kargel., J.S., G.J. Leonard, D.H. Shugar, U.K. Haritashya, A. Bevington, et al. (2015). Geomorphic and geologic controls of geohazards induced by Nepal's 2015 Gorkha earthquake. *Science* **351** (6269), DOI: 10.1126/science.aac8353.

Schultz-Fellenz, E.S., R.T. Coppersmith, A.J. Sussman, E.M. Swanson, and J.A. Cooley (2018). Detecting surface changes from an underground explosion in granite using unmanned aerial system photogrammetry. *Pure and Applied Geophysics* **175**, 3159-3177, https://doi.org/10.1007/s00024-017-1649-0.

Schultz-Fellenz E.S., E.M. Swanson, A.J. Sussman, R.T. Coppersmith, R.E. Kelley, E.D. Miller, B.M. Crawford, A.F. Lavadie-Bulnes, J.R. Cooley, S.R. Vigil, M.J. Townsend, and J.M. Larotonda (2020). High-resolution surface topographic change analyses to characterize a series of underground explosions. *Remote Sensing of Environment* **246**, 111871, https://doi.org/10.1016/j.rse.2020.111871.

Smith, K.D., J.N. Brune, and G. Shields (2000). "A sequence of very shallow earthquakes in the Rock Valley fault zone, southern Nevada Test Site," Chapter L, *U.S. Geol. Open---File Rept. Seismic Hazard Issues Yucca Mountain*.

Smith, M.J., and C.F. Pain (2009). Applications of remote sensing in geomorphology. *Progress in Physical Geography: Earth and Environment* **33** (4), 568-582, https://doi.org/10.1177/0309133309346648.

Tarolli, P., and S.M. Mudd (2020). "Remote Sensing of Geomorphology." Elsevier, 398 p.

USGS (1999). "Digital geologic map of the Nevada Test Site and vicinity, Nye, Lincoln, and Clark Counties, Nevada, and Inyo County, California" *Open-File Report 99–554–A*, 56pp.